Threshold changes in storm runoff generation at a till-mantled headwater catchment

J. M. Detty[1] and K. J. McGuire[2]

[1]   A small research watershed in the Hubbard Brook Experimental Forest in New Hampshire was equipped with a spatially distributed instrument network designed to continuously monitor hydrometric responses in the shallow subsurface. We analyzed rainfall events during seasonal wet up from late summer through autumn to investigate the mechanisms of runoff generation and the patterns of rainfall-runoff response at the catchment outlet. Our results show that storm quick flow depths displayed a threshold relationship with two independently measured soil moisture indices: a maximum water table height index and the sum of gross precipitation and antecedent soil moisture. Quick flow depths during events with below-threshold criteria were not significantly correlated with either index, while quick flow depths during events with above-threshold criteria were strongly correlated with both indices ($r \geq 0.98$). The effective runoff contributing area (estimated by event runoff ratios) also changed significantly between above- and below-threshold conditions, as did the synchronicity between groundwater fluctuations and streamflow. Below the threshold, we inferred that catchment runoff was generated primarily in the near-stream zones, while above the threshold the contributing area likely expanded laterally onto neighboring hillslopes. Our results show that the effective saturated hydraulic conductivity appeared to increase significantly during runoff events with above-threshold conditions, possibly owing to water tables rising into highly transmissive near-surface soils. We believe the observed threshold pattern may partially be explained as a transmissivity feedback mechanism and/or preferential flows through macropore networks which allowed for a rapid expansion of the runoff contributing area onto hillslopes, resulting in increased runoff yields.

1.   Introduction

[2]   One of the great challenges facing catchment hydrology has been the discontinuity between processes observed at the plot or hillslope scale and the integrated effect of processes at the scale of the small catchment [*Bonell*, 1998; *Kirchner*, 2003; *Sivapalan*, 2003; *Tetzlaff et al.*, 2008]. Of particular importance has been linking observed runoff-generating mechanisms with the observed runoff responses at the outlet of a catchment. This is important in the development, application, and evaluation of rainfall-runoff models [*Hooper et al.*, 1998; *Seibert et al.*, 2003], coupled hydrology-ecosystem models [*Band et al.*, 1993], and geomorphology models [*Sidle and Onda*, 2004], which are ultimately used as a basis for making land management decisions and synthesizing our current hydrological understanding.

[3]   The traditional model of streamflow generation in forested catchments suggests that a combination of shallow subsurface stormflow, saturation overland flow, and direct channel interception of rainfall, all expressed as a variable source area model, are primarily responsible for producing a storm hydrograph [*Hewlett and Nutter*, 1970; *Dunne*, 1983; *DeWalle et al.*, 1988; *Wels et al.*, 1991; *McDonnell*, 2003]. This model generally assumes that there are extensive portions of a catchment that frequently saturate to the surface in near-stream regions, thus enabling a rapid and significant stream response to rainfall. However, in many research catchments surface saturation is spatially limited, stream chemistry during runoff events is dominated by previously stored soil water and groundwater (i.e., old water), and storm runoff is controlled by subsurface flows [e.g., *Harr*, 1977; *Bazemore et al.*, 1994; *McGlynn et al.*, 2002; *Williams et al.*, 2002; *Carey and Quinton*, 2005].

[4]   It is obvious that in many catchments, subsurface flows are the dominant processes in generating storm runoff, although explaining how such a rapid and significant "old water" response is translated through the subsurface remains something of a paradox [*Kirchner*, 2003]. In many watersheds, measured saturated hydraulic conductivities significantly underestimate the effective hillslope or catchment scale hydraulic conductivity [e.g., *Binley et al.*, 1989], and

[1]Center for the Environment, Plymouth State University, Plymouth, New Hampshire, USA.
[2]Department of Forest Resources and Environmental Conservation, Virginia Water Resources Research Center, Virginia Polytechnic Institute and State University, Blacksburg, Virginia, USA.

calibrated saturated hydraulic conductivities in rainfall-runoff models are typically much higher than measured values [e.g., *Grayson et al.*, 1992]. Consequently, much research effort has focused on non-Darcian flow in the subsurface by describing soil heterogeneities and preferential flow pathways through macropores and soil pipes which are not typically represented by point measurements of soil hydrologic properties [*Mosley*, 1979; *Sklash and Farvolden*, 1979; *Beven and Germann*, 1982; *McDonnell*, 1990; *Sidle et al.*, 2001]. While many researchers have since observed rapid subsurface flow responses from macropores using tracers [e.g., *Weiler and Naef*, 2003] and hydrometric measurements [e.g., *Uchida et al.*, 1999; *Scherrer et al.*, 2007], most of the research has been confined to the hillslope scale, and there remains a question of how these processes cumulatively affect catchment runoff.

[5] The scale discrepancies inherent to hydrological processes suggest that catchments should be treated as nonlinear systems where changing scales of space and time inevitably change the storages, flow paths, and other subsurface characteristics which control stream runoff [*McDonnell*, 2003]. Recent commentaries suggest that identifying nonlinear controls on runoff generation and patterns of emergent higher-order systems behavior may help to offer insight into the scaling problems confronted by catchment modeling [*McDonnell*, 2003; *Sivapalan*, 2003; *McDonnell et al.*, 2007; *Tetzlaff et al.*, 2008]. Nonlinear or threshold changes in rainfall-runoff response can represent emergent hydrologic behaviors in catchments where processes change dynamically (e.g., activation of runoff-generating mechanisms) and produce changes in runoff responses that are not proportional to forcing inputs across the entire range of inputs [*Phillips*, 2003]. Nonlinear hillslope runoff responses to rainfall have been empirically shown to be sensitive to total precipitation [*Tani*, 1997; *Tromp-van Meerveld and McDonnell*, 2006a, 2006b], antecedent soil moisture storages [*Sidle et al.*, 1995; *Kim et al.*, 2005], and water table elevation [*Kim et al.*, 2004]. Modeling results have also demonstrated that threshold changes in hillslope runoff response could occur with minor variations in storage and connectivity parameters at small spatial scales [*Lehmann et al.*, 2007]. The above examples represent research at the hillslope scale, and the results do not necessarily extrapolate to describe overall catchment behavior [e.g., *Kim et al.*, 2004] and thus highlight the need to identify similar relationships at the scale of a small catchment.

[6] The Hubbard Brook Experimental Forest (HBEF), where this study takes place, is renowned for forest ecosystem research on biogeochemistry [*Likens and Bormann*, 1995], acid rain [*Likens et al.*, 1996], and forest manipulation [*Hornbeck et al.*, 1986, 1997]. In addition, the small-watershed approach to studying nutrient fluxes and cycling was pioneered at HBEF [*Bormann and Likens*, 1967]. Although water flows through the landscape are fundamentally important to much of the research at HBEF, relatively few studies at HBEF have focused on shallow subsurface flow processes or rainfall-runoff relationships. What has been shown in previous research is that the headwater catchments of HBEF seem typical of the small-watershed paradox [*Kirchner*, 2003]. Hydrochemical studies have demonstrated that stormflow, during rain and snowmelt events, was largely composed of rapidly mobilized

"preevent" soil water and shallow groundwater [*Hooper and Shoemaker*, 1986; *Hogan and Blum*, 2003; *Wellington and Driscoll*, 2004]. Likewise, hydrometric studies conducted on select hillslopes also indicate that subsurface stormflow was the primary mechanism for generating streamflow [*Rosenthal*, 1986; *Cedarholm*, 1994]. What has not been resolved at HBEF are the effects of soil moisture storages and event characteristics on runoff, the dominant runoff-generating processes, and the role of hillslopes during runoff events.

[7] In this study, we identify the patterns of rainfall-runoff response of a small forested catchment through the use of a spatially distributed instrument network designed to continuously measure hydrometric responses in the shallow subsurface. We compare our observations against a Darcian framework in order to describe and evaluate rainfall-runoff nonlinearities and potential runoff-generating processes. Ultimately, we sought to answer the following questions: (1) Do threshold patterns in stormflow emerge at the catchment scale resulting from changes in antecedent moisture conditions? (2) What are the inferred contributing areas to storm runoff and how do these change with antecedent conditions and event characteristics? (3) Which runoff-generating processes might sufficiently explain the observed storm runoff response?

2. Site Description

[8] This study took place in watershed 3 (WS3, 42.4 ha, Figure 1) in the Hubbard Brook Experimental Forest located near West Thornton, New Hampshire. WS3 is the hydrologic reference watershed for a series of paired watershed studies at HBEF [*Federer*, 1969; *Likens et al.*, 1970; *Hornbeck et al.*, 1970; *Hornbeck*, 1975, 1973]. The catchment is underlain by the upper and lower Rangeley Formation, a pelitic schist. The surficial geology has been largely shaped by the sequence of Pleistocene glaciations, with the latest Wisconsinan glacial period having deposited a layer of basal and ablation tills of varying thickness [*Johnson et al.*, 2000]. Soils in this area comprise ~80% Spodosols (haplorthods) with well-developed horizons, a characteristic eluviated layer, and a predominant B horizon with sesquioxide coatings. The remaining ~20% of soils are Inceptisols with no or poorly developed spodic horizons. These soils feature a thick organic horizon on top of a mineral horizon derived from basal till parent material with a large proportion of boulders and rock fragments. A defining feature of these soils is a very tight densipan C horizon (Cd) encountered at ~70 cm which is composed of compacted silt loam tills. Macropores and soil pipes are a common feature of the organic soil horizons, and *Stresky* [1991] found that total soil pipe volume decreased with depth from an average of 0.75% of the Oa horizon to 0.049% of the Bs horizon. Soil infiltration rates are very high, on the order of meters per day (C. A. Federer, Soil water properties and data for the Hubbard Brook Experimental Forest, unpublished report, 1992), and are typically well in excess of precipitation rates.

[9] The climate of HBEF is humid continental with an average January temperature of −9°C and an average July temperature of 18°C with an even distribution of precipitation throughout the year. About one quarter to one third of the 1400 mm of annual precipitation occurs as snow, and
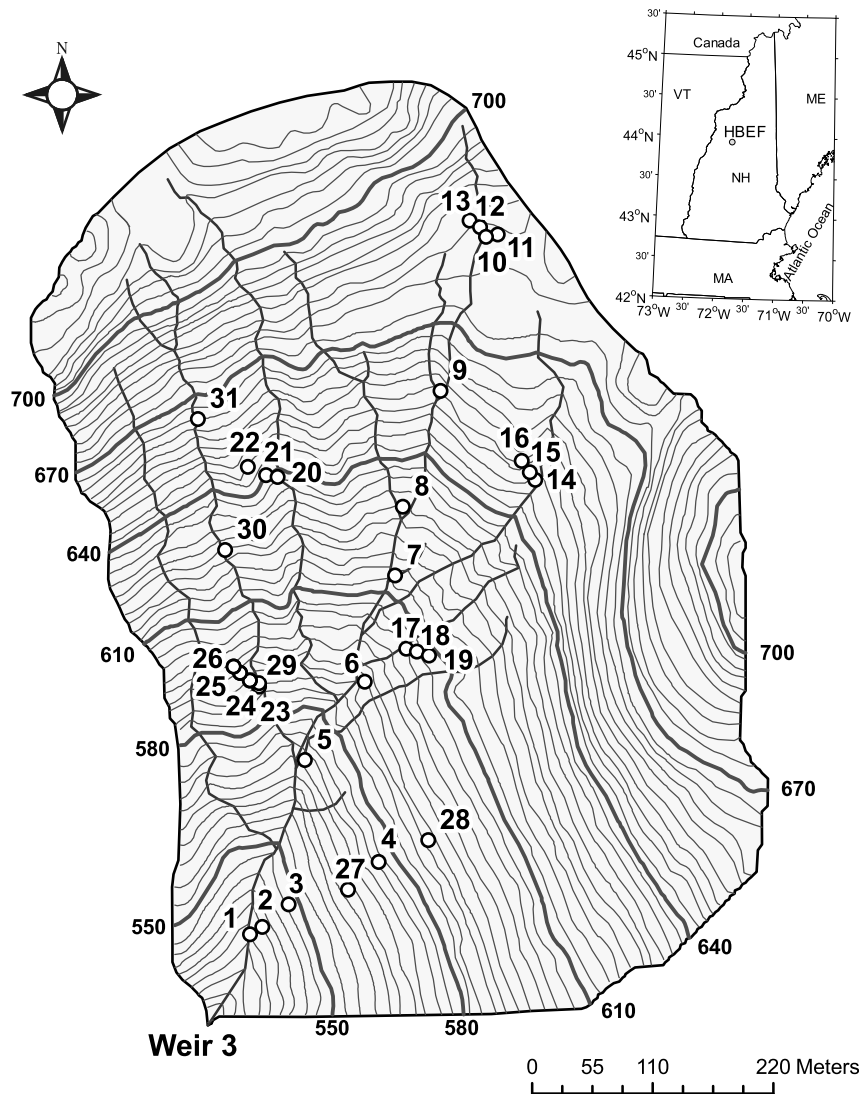
Figure 1. Site map of watershed 3. Contour interval is 3 m. Numbers and circles correspond with well numbers and locations. Soil moisture sensors are located adjacent to wells 23–26. Rain gauge 1 is not visible on the map and is located 450 m SSW of weir 3. Inset map shows the general location of the Hubbard Brook Experimental Forest (HBEF).

nearly half of the 870 mm of annual runoff occurs during the spring snowmelt period [*Bailey et al.*, 2003].

[10] WS3 has a southerly exposure and an elevation range of 527–732 m. The catchment is completely forested with typical northern hardwood species, primarily American beech (*Fagus grandifolia*), sugar maple (*Acer sacharum*), and yellow birch (*Betula alleghaniensis*). On the ridgetops, balsam fir (*Abies balsamea*), red spruce (*Picea rubens*), and white birch (*Betula papyrifera* var. *cordifolia*) are common [*U.S. Department of Agriculture Forest Service*, 1996]. A good general description of this site is given by *Likens and Bormann* [1995].

3. Methods

3.1. Field Design and Instrumentation

[11] Our study featured a spatially distributed instrument network which was designed to represent the hydrometric responses of the shallow subsurface throughout the catch-

ment. We installed instrument transects that represent the range of typical local landform shapes that define the catchment: concave footslopes (near-stream areas), planar back slopes (hillslopes or side slopes), and convex shoulders (divergent areas). We installed 28 shallow groundwater wells (wells 1–28 in Figure 1) and three stream stage recorders (wells 29–31 in Figure 1) in WS3.

[12] Each well was constructed of SDR 21 PVC pipe (3.18 cm OD) with a 31 cm screen length consisting of 0.025 cm width lateral slots with 0.32 cm spacing between slots. The wells were installed by boring a hole with a 10 cm diameter hand auger, inserting the pipe, and then backfilling around the pipe. A 2 cm layer of coarse bentonite was added at the top of the mineral soil horizon before replacing the organic soil and root mat around the pipe. The wells were installed to a depth of ~10 cm into the compact Cd soil horizon or where there was no Cd horizon to a depth of tool refusal for a total depth of 71–118 cm for all wells. Each well was equipped with a water level recorder (Odyssey
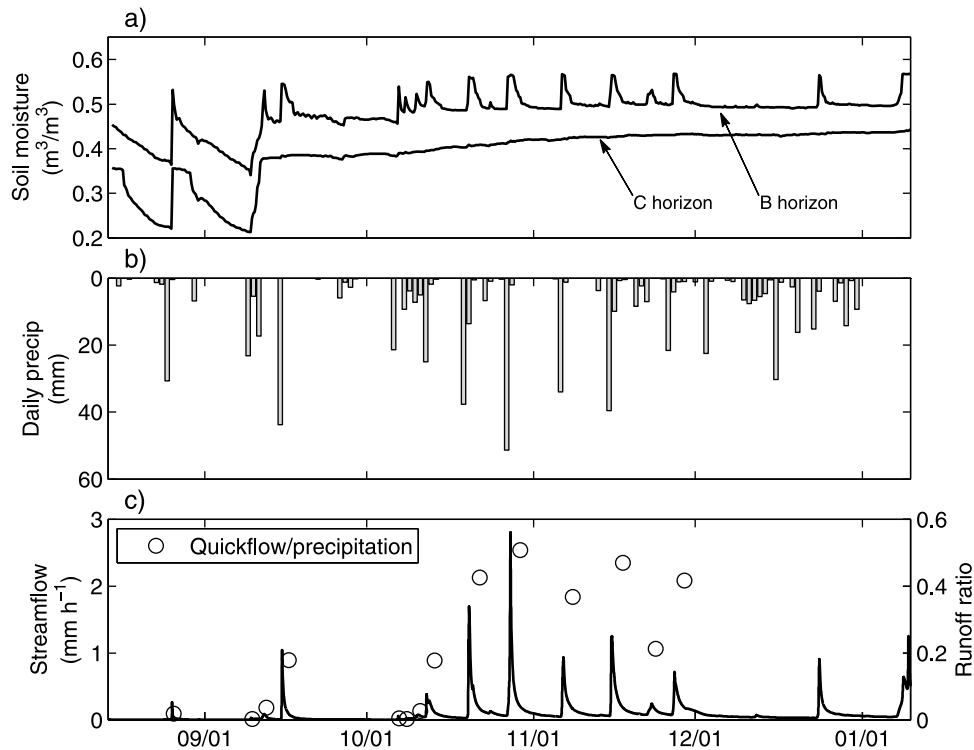
Figure 2. Overview of study period. The dry and transition periods coincided with the growing season, and the wet period coincided with the dormant season. (a) Volumetric water content for the lower B horizon (45 cm) and the C horizon (61 cm) at well 23. Well 23 shows the strongest seasonal patterns and therefore was selected for this graphic. Only data from two sensors are shown for graphical clarity. (b) Daily precipitation at rain gauge 1. (c) Streamflow at weir 3 and runoff ratios (quick flow/precipitation) for rainfall events at WS3.

Capacitance Water Level Logger 1.5 m) which uses a capacitance measurement to determine the wetted length of flexible Teflon®-coated wire that is suspended freely in the pipe. Each device was set to record at 10 min intervals, and we obtained a continuous record from August 2007 through January 2008.

[13] At wells 23–26 (see Figure 1), we supplemented the four monitoring wells with a series of electronic soil moisture sensors (Decagon Devices EC-5). The sensors measure the dielectric constant of the soil to determine the volumetric water content [*Kizito et al.*, 2008]. Five sensors were installed at discrete depths in the soil profile ~1.5 m downslope of each of the four monitoring wells (total of 20 sensors). Sensors were installed by digging a soil pit to the C horizon, which at well 23 was a gravelly buried alluvium, at wells 24 and 25 was a firm densipan horizon, and at well 26 was a less compact till-derived C horizon. Sensors were installed with the prongs oriented horizontally in the lower Oa horizon, the A/B interface, the upper B horizon, the lower B horizon, and the upper C or Cd horizon. After installation, the pit was backfilled with the excavated soils. We utilized the default factory calibration for all sensors, and each group of sensors was connected to a Decagon Devices Em50 data logger and set to record at 10 min intervals for the study period.

3.2. Study Period

[14] We present results from 14 August 2007 through 10 January 2008 (Figure 2). Soil moisture data were con-

tinuous throughout the entire study period; however, well data were only continuous after 1 September 2007, and any well data prior to that date have been omitted from our analyses. Events with snowfall and/or snowmelt were excluded from all analyses involving the precipitation data because of the uncertain and heterogeneous inputs from those events. The resulting study period included 14 separate rainfall events of at least 9 mm (Table 1). All rainfall data were measured at rain gauge 1, and all runoff data were measured at weir 3 (see Figure 1); both were measured and archived by the U.S. Department of Agriculture (USDA) Forest Service (publicly available at http://hubbardbrook. org). In all of the analyses presented, streamflow refers to total streamflow as measured at weir 3, while quick flow (also referred to as stormflow) was determined using the constant slope hydrograph separation method of *Hewlett and Hibbert* [1967].

3.3. Saturated Hydraulic Conductivity Estimates

[15] We performed slug tests in 11 of the 28 groundwater wells to calculate saturated hydraulic conductivity of the integrated soil profile according to the Hvorslev method for a rising head test [*Weight and Sonderegger*, 2001]. These tests were performed during the end of spring snowmelt in April 2008 when water tables were generally high. However, groundwater levels during large runoff events did exceed the levels at which the slug tests were performed; therefore, the slug tests could not represent the uppermost

Table 1. Event Characteristics for Watershed 3[a]

Event	Date	Event Duration (days)	P_{gross} (mm)	P_{avg} (mm/h)	P_{max} (mm/h)	TF (mm)	QF (mm)	RR	ASI (mm)	$\sum$(ASI and P_{Gross}) (mm)	H_{max}
					Below-Threshold Events						
1	25 Aug 2007	0.6	31.8	2.7	12.4	28.5	0.6	1.9%	245	277	–
2	9 Sep 2007	0.6	31.2	1.2	7.8	28.0	0.1	0.2%	240	272	0.11
3	11 Sep 2007	1.0	17.0	1.2	4.8	15.2	0.6	3.6%	278	295	0.33
5	6 Oct 2007	0.7	23.4	1.6	8.8	21.0	0.1	0.5%	268	291	0.28
6	8 Oct 2007	0.5	10.2	1.3	5.9	9.1	0.0	0.3%	286	297	0.31
7	9 Oct 2007	1.1	13.2	0.7	1.6	11.8	0.4	2.7%	290	303	0.38
					Above-Threshold Events						
4	15 Sep 2007	1.6	48.0	2.7	12.7	43.1	8.5	17.8%	279	327	0.59
8	11 Oct 2007	1.8	30.2	1.2	7.2	27.1	5.4	17.8%	300	331	0.56
9	19 Oct 2007	2.4	54.9	1.5	10.4	51.7	23.4	42.6%	298	353	0.80
10	26 Oct 2007	2.6	56.8	1.6	8.2	53.5	28.8	50.8%	307	364	0.92
11	6 Nov 2007	2.3	38.1	2.7	7.2	35.9	14.0	36.7%	302	340	0.71
12	15 Nov 2007	2.5	45.4	1.1	13.7	42.8	21.3	46.9%	309	354	0.76
13	21 Nov 2007	2.2	9.5	0.3	1.5	8.9	2.0	21.2%	308	317	0.51
14	26 Nov 2007	2.4	25.9	2.0	3.6	24.4	10.8	41.6%	308	334	0.67

[a]TF, throughfall estimate based on the work by *Leonard* [1961a, 1961b]; QF, quick flow estimate [*Hewlett and Hibbert*, 1967]; RR, runoff ratio of quick flow/gross precipitation; ASI, antecedent soil moisture index; H_{max}, maximum water table height index.

soil horizons into which water tables briefly rose during the largest events.

[16] We also compared the slug test data with extensive independent estimates of saturated hydraulic conductivity (82 total) obtained from a constant head permeameter [*Amoozegar*, 1989] at multiple depths and multiple locations throughout WS3. In addition, we compared our K_{sat} estimates with data from slug tests and a tracer experiment performed at a hillslope ~30 m south of weir 3 [*Cedarholm*, 1994] as well as a nearby site in the Mirror Lake basin [*Shattuck*, 1991]. All of the K_{sat} estimates for soils above the

till interface (O/A through lower B horizons) spanned comparable ranges and were typically on the order of ~10^{-3} to 1 m/d.

4. Results

4.1. Nonlinear Hydrologic Characteristics

[17] In WS3, we found that event quick flow depths were correlated with antecedent soil moisture and gross precipitation (Figure 3). We determined an antecedent soil moisture index (ASI) from the four instrumented soil profiles located
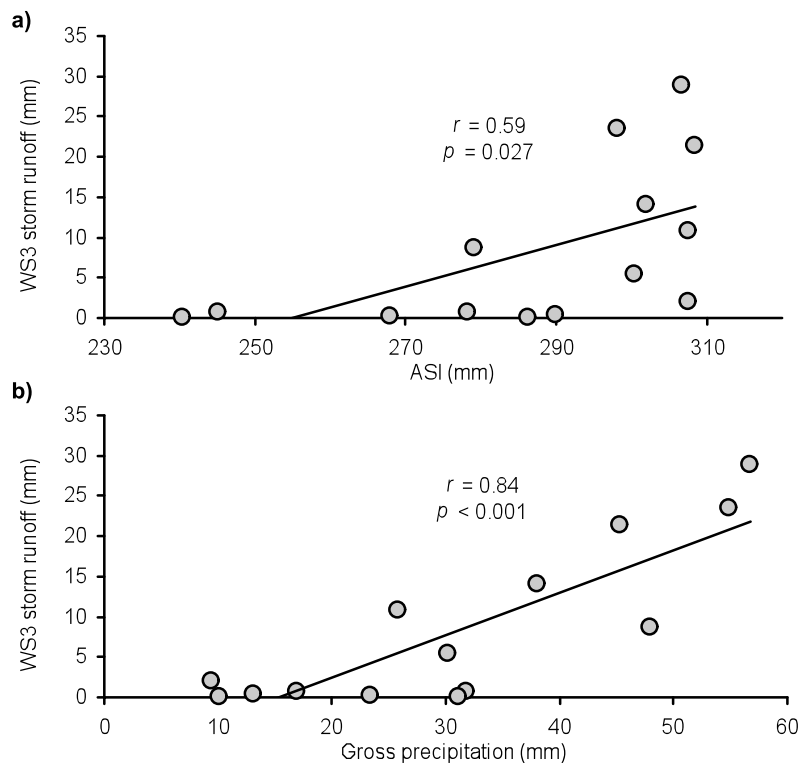

Figure 3. Soil moisture, gross precipitation, and total quick flow runoff depths. (a) Quick flow for all events and an antecedent soil moisture index (ASI). (b) Quick flow for all events and total gross precipitation.
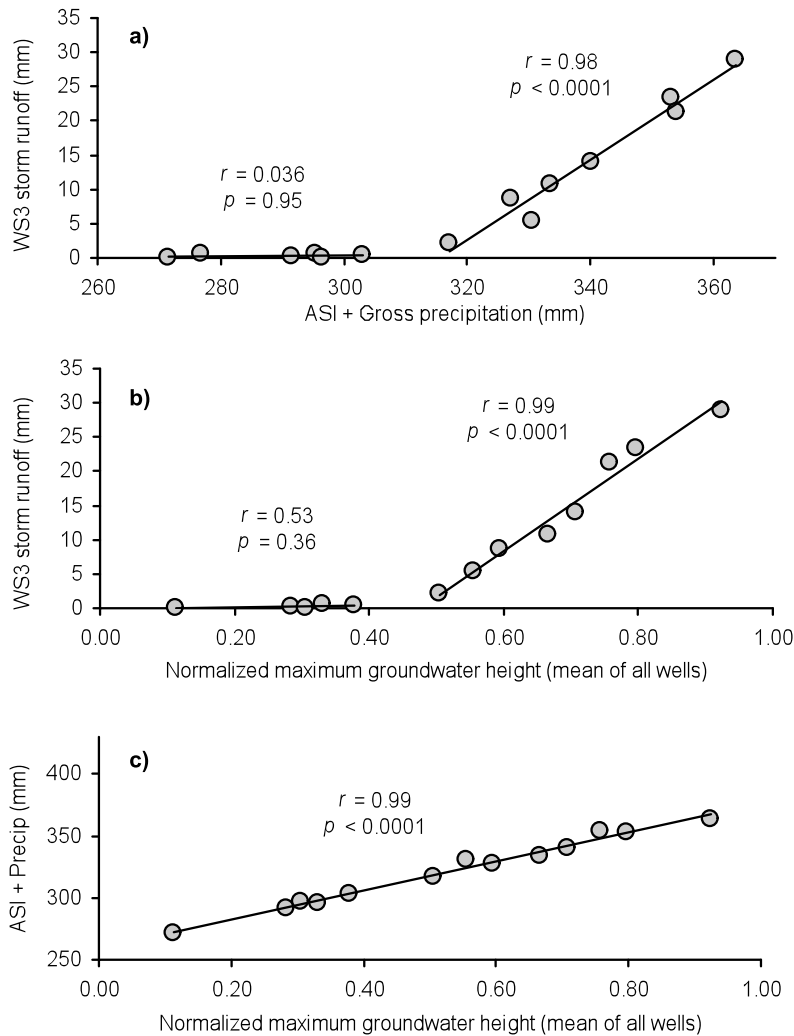
Figure 4. Soil moisture indices and total quick flow runoff depths. (a) Quick flow for all events and the sum of total gross precipitation and an antecedent soil moisture index. Threshold value is ~316 mm. (b) Quick flow for 13 of 14 events (event 1 has been omitted) and the mean of maximum event water table heights for all wells. Water table heights were normalized to measured seasonal ranges (1 is maximum, 0 is minimum or lowest recordable depth). Threshold value is ~0.48. (c) The sum of total gross precipitation and ASI and maximum event water table height for 13 of 14 events (event 1 has been omitted).

at wells 23–26 in Figure 1 using a method developed from *Haga et al.* [2005]. The soil moisture data immediately preceding an event were used to determine the total soil water content at each profile from the sum of water content in each soil horizon (where water content is the integration of volumetric water content over the depth interval represented by each soil moisture sensor). We then used the arithmetic mean of the total water content at the four profiles to determine ASI. Correlations among other variables such as average and maximum precipitation intensity, runoff ratios (Table 1), and antecedent streamflow were also considered; however, the correlations were not as strong as with ASI and gross precipitation. When ASI and gross precipitation were summed and compared to total event quick flow, a clear threshold pattern was evident (Figure 4a). Below a threshold value of ~316 mm, the relationship between the sum of ASI and gross precipitation and total quick flow was poorly correlated ($r = 0.036$, $p = 0.95$). Above this value,

however, the relationship was highly correlated ($r = 0.98$, $p < 0.0001$).

[18] A maximum water table height index was also calculated for each event by normalizing the water level in each well to its measured seasonal range, then obtaining the maximum instantaneous value for each well for each event, and calculating the arithmetic mean of maximum heights for all wells during each event (except for event 1, which was omitted from this analysis because of only 20 of the 28 groundwater wells being operational at that time). In instances where the water level dropped below the lowest measurable depth of an instrument, typically at the B/C interface, we assigned a value of zero to those data, as our interest was in characterizing shallow flow processes above the basal till horizon. We believe that normalizing and averaging the data in this way, and thus weighting each well equally, gives a better index of how shallow groundwater across the entire catchment was responding than would
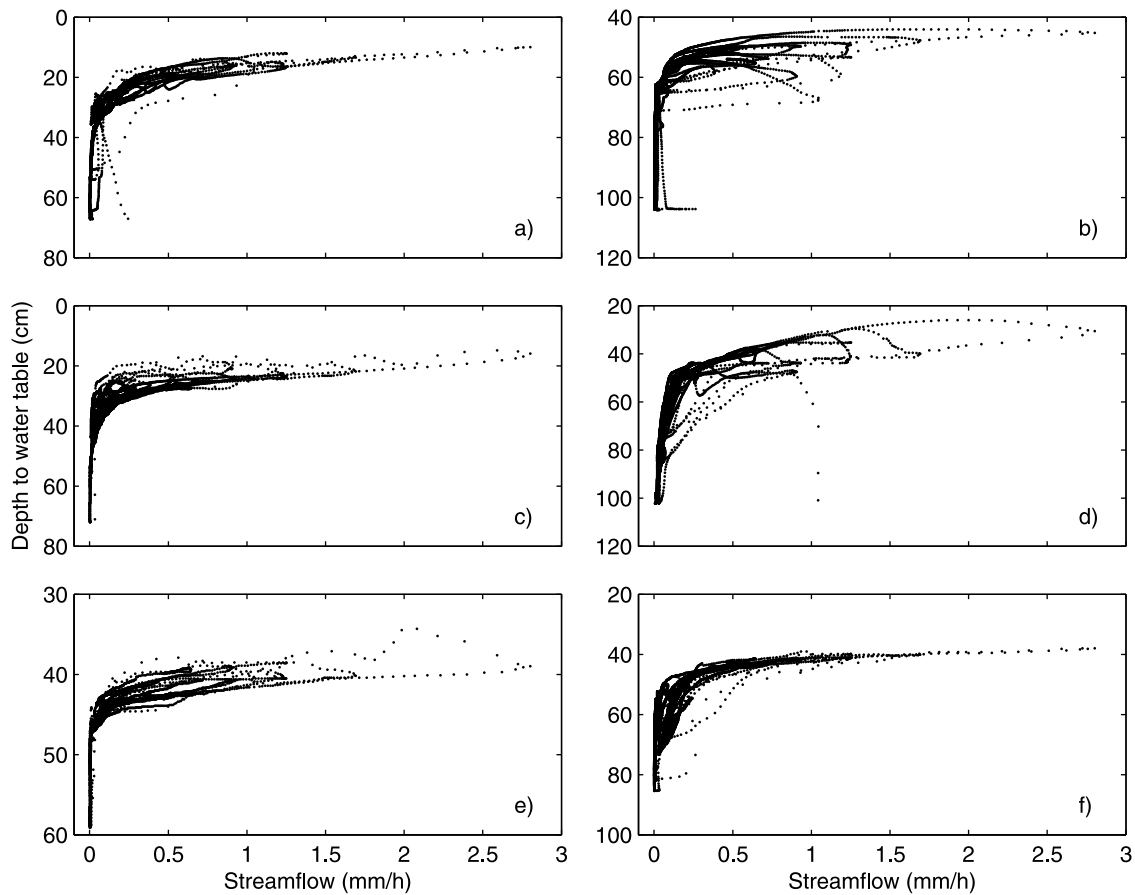
Figure 5. Depth to groundwater and streamflow for six hillslope wells for the entire study period. Markers were plotted at 10 min intervals: wells (a) 2, (b) 8, (c) 14, (d) 19, (e) 20, and (f) 25.

absolute measurements, which would bias the wells with larger groundwater fluctuations. A threshold pattern very similar to Figure 4a is evident by comparing event quick flow volumes with maximum water table height (Figure 4b). Comparing ASI and gross precipitation to maximum water table height (Figure 4c) shows that the two metrics were highly correlated ($r = 0.99$, $p < 0.0001$). It is worth noting that for these analyses, ASI, which was calculated from four instrument locations on one hillslope (wells 23–26 in Figure 1), and the maximum water table height index, which was determined from all groundwater wells throughout WS3 (wells 1–28 in Figure 1), offer independent but complimentary results.

[19] Many of our wells, both near-stream and hillslope, also showed a curvilinear relationship between groundwater heights and streamflow both in the entire record and during events. These patterns suggest an inflection point above which minor changes in water table height were associated with large changes in stream discharge (Figure 5) and below which large changes in water table height were associated with minor changes in stream discharge. The depth at which the inflection point occurred varied between wells but was typically encountered between 20 and 50 cm below the ground surface. Although these patterns were fairly consistent throughout the study period, there were some outlier data (e.g., Figure 5b) that did not conform to the general curvilinear patterns, emphasizing the dynamic and variable nature of groundwater responses.

4.2. Hillslope Groundwater Responses

[20] The ratio of storm quick flow to precipitation is a commonly used estimate of the effective contributing area during a runoff event [*Hewlett and Hibbert*, 1967; *Dickinson and Whiteley*, 1970; *Harr*, 1977; *Turton et al.*, 1992; *Buttle et al.*, 2004]. Our site surveying suggested that in watershed 3, the channel network represented ~1.8% of the total catchment area, and the near-stream toe slopes (within ~10 m of the channel) represented ~10% of the total catchment area. Therefore, when runoff ratios rose above ~12% (runoff ratios varied from 0.2% to 51% for this study, see Table 1), we inferred that the effective contributing area expanded onto the hillslopes. Our well hydrograph data support this inference with evidence that hillslope groundwater responses became increasingly synchronized with streamflow as event runoff ratios increased.

[21] We calculated Spearman's rank correlation [*Noether*, 1991] between streamflow and water table heights for all wells during all events to determine the synchronicity of groundwater and streamflow responses throughout the catchment. Rank correlation was chosen because it is a nonparametric measure and our data distributions were highly nonnormal. There is a clear pattern of decreasing rank correlation with distance from the channel when all events were considered (Figure 6). However, by binning the data by runoff ratio and considering only the hillslope wells (Figure 7a), there was also a pattern of increasing correlation
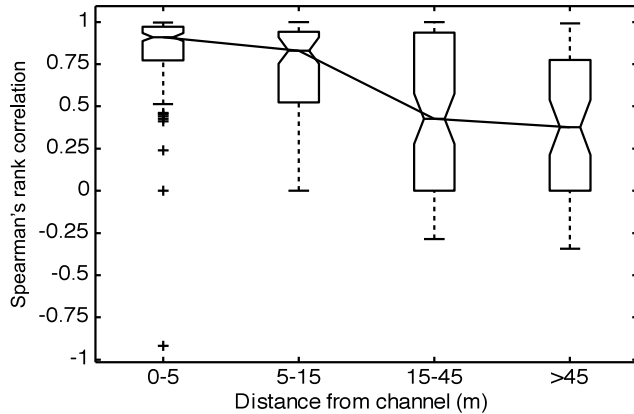
Figure 6. Box plot of Spearman's rank correlation between groundwater levels and streamflow for all wells and all events. Boxes represent the interquartile range (IQR) of data, and notches represent the 95% confidence limit of the median values. Whiskers describe the highest and lowest nonoutlier data. Outliers are defined as any data greater than 1.5 times IQR plus the third quartile or less than the first quartile minus 1.5 minus IQR. Wells with no groundwater response during events were inferred to be uncorrelated with streamflow and were assigned a rank correlation of 0.

between hillslope water table fluctuations and streamflow for increasing runoff ratios. Events with runoff ratios above 0.2 had hillslope well hydrographs that were highly correlated with streamflow (median value is 0.88), while events with runoff ratios below 0.2 had hillslope well hydrographs that were far less correlated with streamflow (median value is 0). We also evaluated the synchronicity between hillslope groundwater and streamflow by calculating the time lags between streamflow response and groundwater responses during events using Spearman's best fit lag analysis [*Hjerdt*, 2002; *Seibert et al.*, 2003]. In this analysis, Spearman's rank correlation coefficient was used to objectively determine the time lags between streamflow and groundwater levels. This was computed by lagging the groundwater data set at 1 h intervals from −7 to +24 h to determine the highest rank correlation coefficient, which was considered the effective time "lag." Although hillslope time lags were not significantly correlated with runoff response, the variability of lag times decreased as runoff ratios increased (Figure 7b). In addition, groundwater level variance throughout the catchment, expressed as the interquartile range of normalized groundwater levels, also decreased as maximum groundwater levels increased (a surrogate for increased soil moisture) (Figure 8). These results suggest that groundwater responses on hillslopes became more homogeneous and synchronized with streamflow as the catchment runoff response increased.

4.3. Estimated Contributing Areas and Subsurface Stormflow

[22] For each event we calculated an estimated contributing area on the basis of Darcy velocities and compared the results with runoff ratios to evaluate the representativeness

of our field measurements and to test whether a Darcian framework could explain the observed runoff response. An event subsurface flow distance based on Darcy velocity and event duration was estimated as

$$D_{SSF} = \sum_{t=1}^{n} K_{sat}[h(t)]\tan\beta\Delta t, \qquad (1)$$

where $K_{sat}(h)$ is the average saturated hydraulic conductivity of the soil profile which varies with groundwater levels (based on an exponential relationship determined from the extensive permeameter data in WS3, shown in Figure 9, and adapted to slug test results for each well), $h(t)$ is the height of the water table at time t, $\tan \beta$ is the hydraulic gradient (assumed to be parallel to the local land surface), and Δt is the integration time step. We calculated D_{SSF} at a 10 min time step for the duration of each event (i.e., from $t = 1$ to $t = n$). For this exercise, we assumed that the estimated total contributing area was equal to the sum of contributing areas for each stream reach. As a first
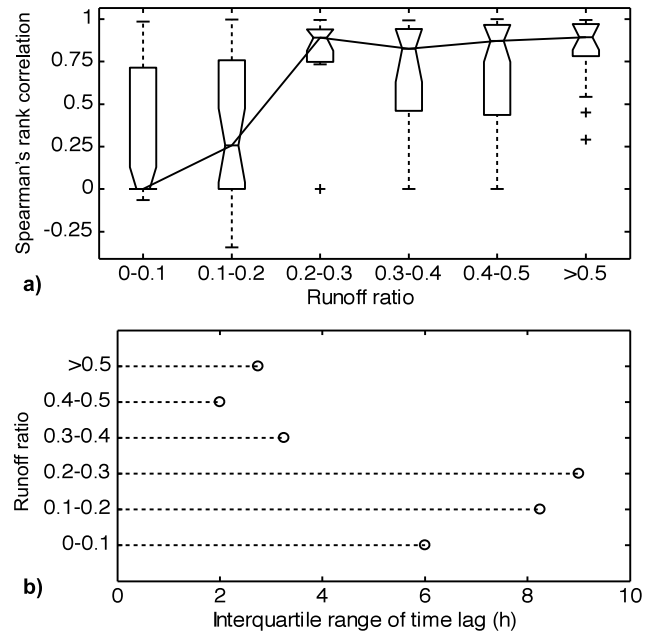

Figure 7. Hillslope groundwater and streamflow correlations. (a) Box plot of Spearman's rank correlation between groundwater levels and streamflow for all hillslope wells and all events. Boxes represent the IQR of data and notches represent the 95% confidence limit of the median values. Whiskers describe the highest and lowest nonoutlier data. Outliers are defined as any data greater than 1.5 times IQR plus the third quartile or less than the first quartile minus 1.5 minus IQR. Wells with no groundwater response during events were inferred to be uncorrelated with streamflow and were assigned a rank correlation of zero. (b) Dot plot of the IQR of Spearman's best fit lag times for all hillslope wells and all events. Lag times were calculated for each well and event by advancing the groundwater data set at a 1 h interval from −7 to +24 h and computing rank coefficients for each time step to determine the most correlated time lag. Wells with no groundwater response were omitted from this analysis.
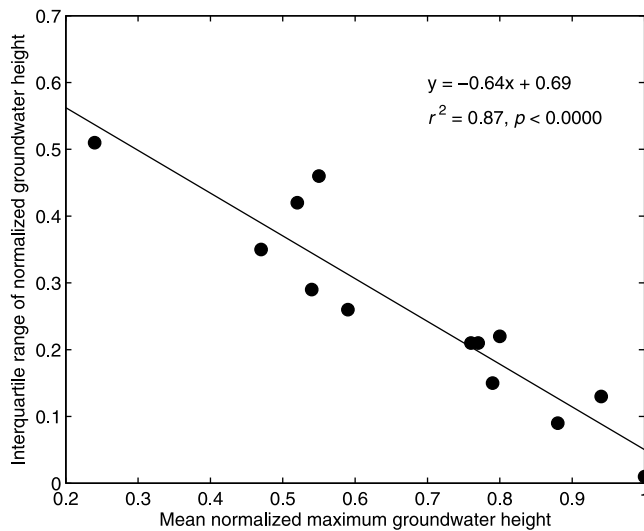
Figure 8. Mean normalized maximum groundwater height and interquartile range of normalized groundwater height. Groundwater data were normalized to the observed seasonal range (1 is maximum and 0 is minimum or lowest record-able depth). The maximum instantaneous value for each well for each event was determined and reported as the arithmetic mean of all wells for each event.

approximation, each stream reach was represented as a linear channel, with planar hillslopes on both sides of the channel and where flow paths were oriented perpendicular to the stream channel. We assumed that runoff was generated only via direct channel interception and Darcian flow through the soil matrix. D_{SSF} was determined for each well and event, and the largest D_{SSF} within a reach segment was assigned to the entire reach segment for that event (i.e., to represent the largest contributing area that could occur within a given reach for a given event on the basis of measured well data). Stream segments that were not instrumented were assigned the largest D_{SSF} from the nearest neighboring instrumented stream reach for each event. We then defined the estimated contributing area as

$$A_c = \sum_{i=1}^{10} ([2D_{SSF}l] + A_{ch}), \qquad (2)$$

where i is the reach number (the channel network was divided into 10 reach segments), D_{SSF} is the subsurface flow distance discussed above, l is the reach length, and A_{ch} is the channel area for a given reach.

[23] This exercise represents the largest hypothetical contributing area that could be obtained for a given event on the basis of field measurements and assuming Darcian matrix flow through the subsurface. Our results show that for five of the six events with below-threshold criteria, our estimated contributing area was greater than the runoff ratio, while for the eight events with above-threshold criteria and one of the six events with below-threshold criteria, the runoff ratio was greater than our estimated contributing area (see Table 2). While the Darcy velocity estimates were sufficiently high to theoretically explain runoff contributing areas for most below-threshold events, the Darcy velocities would need to be up to an order of magnitude higher for our

estimated contributing areas to equal the runoff ratios of the above-threshold events.

[24] We also tested Darcy assumptions using our well data and K_{sat} estimates to calculate lateral subsurface flow through near-stream wells during each event. We present the data from the four near-stream wells in which slug tests were performed (1, 17, 20, and 23 in Figure 1), as we felt that the near-stream sites would be most representative of subsurface flows entering the stream channel and because any other near-stream subsurface flow estimates would not be based on site specific K_{sat} data. Subsurface flows were estimated by integrating the area of a well hydrograph (to the level of the preevent water table) for the duration of an event. We assumed that the hydraulic gradient remained parallel to the land surface and that lateral subsurface flow was controlled by the height and duration of the water table. The lateral subsurface flow of water through a well (on a specific area basis) was characterized as

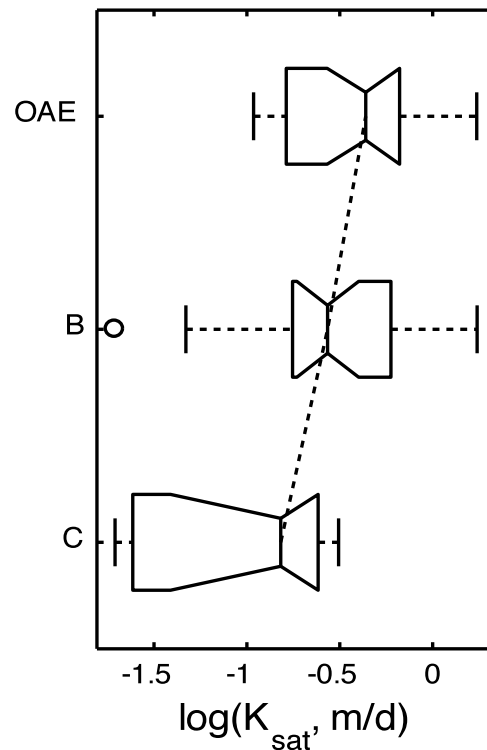$$q_L = \sum_{t=1}^{n} [h(t) - h_a] K_{sat}[h(t)] \tan \beta \Delta t \varphi 2l / A, \qquad (3)$$

Figure 9. Box plot of saturated hydraulic conductivity in the soil profile. Boxes have been binned by soil horizon and the vertical axis is not scaled to depth. Median depths for each horizon are 15 cm for Oa, A, and E (combined), 47 cm for B, and 77 cm for C. Eighty-two measurements are represented and taken from a constant head permeameter in soil boreholes. Boxes represent the IQR of data, and notches represent the 95% confidence limit of the median values. Whiskers describe the highest and lowest nonoutlier data. Outliers are defined as any data greater than 1.5 times IQR plus the third quartile or less than the first quartile minus 1.5 minus IQR.

Table 2. Contributing Area Estimates and Lateral Subsurface Flow Estimates for Four Near-Stream Wells in Watershed 3[a]

| | | | | | | Lateral Subsurface Flows | | | | |
| | | | | | | Well 1 | Well 17 | Well 20 | Well 23 | SSF$_c$ |
Event	Date	P_{gross} (mm)	QF (mm)	RR	A_c	(mm)	(mm)	(mm)	(mm)	(mm)
				Below-Threshold Events						
1	25 Aug 2007	31.8	0.6	1.9%	2.7%	0.08	-	0.29	0.09	0.10
2	9 Sep 2007	31.2	0.1	0.2%	2.6%	0.00	-	0.11	0.00	<0
3	11 Sep 2007	17.0	0.6	3.6%	3.3%	0.08	0.02	0.06	0.22	0.35
5	6 Oct 2007	23.4	0.1	0.5%	2.8%	0.02	0.00	0.11	0.10	<0
6	8 Oct 2007	10.2	0.0	0.3%	2.6%	0.01	0.01	0.01	0.03	<0
7	9 Oct 2007	13.2	0.4	2.7%	3.7%	0.15	0.06	0.06	0.10	0.14
				Above-Threshold Events						
4	15 Sep 2007	48.0	8.5	17.8%	4.5%	0.56	0.33	0.22	0.86	7.79
8	11 Oct 2007	30.2	5.4	17.8%	5.1%	0.36	0.29	0.20	0.25	4.89
9	19 Oct 2007	54.9	23.4	42.6%	6.4%	0.93	0.62	0.39	0.80	22.50
10	26 Oct 2007	56.8	28.8	50.8%	6.7%	1.02	0.52	0.40	0.66	27.90
11	6 Nov 2007	38.1	14.0	36.7%	5.9%	0.60	0.46	0.29	0.49	13.40
12	15 Nov 2007	45.4	21.3	46.9%	6.4%	0.71	0.50	0.36	0.49	20.60
13	21 Nov 2007	9.5	2.0	21.2%	5.4%	0.16	0.16	0.12	0.09	1.86
14	26 Nov 2007	25.9	10.8	41.6%	6.1%	0.51	0.30	0.32	0.28	10.40

[a]QF, quick flow estimate [*Hewlett and Hibbert*, 1967]; RR, runoff ratio of quick flow/gross precipitation; A_c, contributing area estimate as discussed in section 4.3; SSF$_c$, average subsurface stormflow throughout the catchment (equation (4)). SSF$_c$ < 0 indicates events with a channel interception estimate that was greater than observed quick flow.

where $h(t)$ is water table height at time t, h_a is the water table height immediately prior to the start of precipitation, $K_{sat}(h)$ is the average saturated hydraulic conductivity of the soil profile with a water level at height h, $\tan \beta$ is local slope gradient, Δt is the time step interval, φ is porosity (estimated at 0.5 [*Cedarholm*, 1994; C. A. Federer, unpublished report, 1992], l is the total catchment channel length, and A is the catchment area. For this analysis, q_L was integrated at a 10 min time step until the end of quick flow, i.e., when $t = n$.

[25] Assuming that the lateral subsurface flow of water through near-stream wells was comparable to the discharge of water into the nearby stream channel during events, we can evaluate our lateral subsurface flow estimates by comparing them to the catchment-wide average subsurface stormflow during each event. The average catchment subsurface stormflow was estimated for each event by subtracting the direct channel interception volume from the total storm quick flow volume and normalizing to the total catchment area:

$$SSF_c = (V - [A_{ch}TF])/A, \qquad (4)$$

where V is the total quick flow volume, A_{ch} is the total channel area, TF is estimated throughfall based on the throughfall and gross precipitation regressions developed by [*Leonard*, 1961a, 1961b], and A is the total catchment area. This calculation results in an estimation of subsurface stormflow volume per unit area which can be directly compared with the results from equation (3).

[26] This exercise shows that for the below-threshold events one or more near-stream wells had estimated lateral subsurface flows that were comparable to or greater than the catchment average subsurface stormflow (Table 2). However, the above-threshold events showed a very different runoff response as the catchment average subsurface stormflow was approximately 10–100 times greater than our lateral subsurface flow estimates in near-stream wells (Table 2). These results are in agreement with our findings from the contributing area exercises and suggest that subsurface

stormflow in this catchment changes characteristically between above- and below-threshold conditions.

5. Discussion

5.1. Hydrologic Thresholds

[27] In WS3, quick flow depths displayed a consistent threshold response to maximum catchment water table heights as well as the sum of antecedent soil moisture and gross precipitation. Below the threshold, quick flow was not significantly correlated to either of these indices, while above the threshold the relationship between quick flow and each index was linear and significantly correlated. Similar threshold runoff responses have been observed in other studies and have been theorized to reflect soil moisture storage characteristics, hillslope drainage efficiency, saturated area connectivity, and runoff-generating processes [*Sidle et al.*, 1995; *Tani*, 1997; *Buttle et al.*, 2004; *Kim et al.*, 2005; *Tromp-van Meerveld and McDonnell*, 2006a, 2006b; *Fujimoto et al.*, 2008].

[28] Compared to above-threshold events, the below-threshold events in this study typically had spatially limited shallow water tables, greater depths to the water table surface, and drier antecedent soil conditions. Therefore, the runoff response likely reflected a soil moisture storage threshold below which inputs replenished storage deficits and above which inputs were increasingly transferred to lateral subsurface stormflow and catchment runoff. It has long been recognized that antecedent soil moisture and soil storage capacity are strong controls on runoff response [*Kohler and Linsley*, 1951; *U.S. Soil Conservation Service*, 1969; *Lynch et al.*, 1979; *Sidle et al.*, 1995], and some studies have linked these parameters to a threshold change in total stormflow [*James and Roulet*, 2007; *Redding and Devito*, 2008]. At a hillslope site in the Panola Mountain Research Watershed in Georgia, *Tromp-van Meerveld and McDonnell* [2006a, 2006b] noted a threshold subsurface stormflow response to rainfall in an analysis of 147 events. *Lehmann et al.* [2007] used percolation theory to show that the threshold behavior at Panola was sensitive to variations

in soil moisture storages and flow path connectivity at small scales.

[29] At WS3, the relationship between the spatial mean groundwater levels and groundwater level interquartile range (Figure 8) suggests that as the catchment became wet and more spatially uniform, the flow paths became more connected. While other investigators have observed a maximum soil moisture variance at intermediate spatial mean soil moisture [*Western et al.*, 2003; *Pan and Peters-Lidard*, 2008; *Penna et al.*, 2009], the relationship between these variables in our system appears to be more linear.

[30] The observed runoff responses also likely represented a source area threshold and a transition between runoff generated in the near-stream zones during below-threshold events (runoff ratios <4%, hillslope groundwater responses decoupled from streamflow) and increasing hillslope contributions during above-threshold events (runoff ratios >10%, hillslope groundwater responses increasingly synchronized with streamflow). These observations are supported by other research which has shown that threshold increases in runoff are related to increased connectivity of saturated subsurface areas [*Sidle et al.*, 2001; *Tromp-van Meerveld and McDonnell*, 2006a; *Lehmann et al.*, 2007] and subsequent expansion of the contributing area [*Dickinson and Whiteley*, 1970; *Kim et al.*, 2005; *Fujimoto et al.*, 2008]. At the Blue Springs Creek International Hydrological Decade Research Basin in Ontario, Canada, *Dickinson and Whiteley* [1970] found a threshold relationship between runoff and a "basin moisture index," similar to what we present in Figure 4a, and inferred that the runoff response reflected changes in soil storage capacity, drainage characteristics, and contributing area.

5.2. Darcian Matrix Flow Estimates

[31] At HBEF we have multiple independent assessments of saturated hydraulic conductivity (K_{sat}) in the soil profile spanning comparable ranges of ~10^{-3} to ~1 m/d. We used a Darcian framework to estimate contributing areas and lateral subsurface flows primarily as a means of evaluating our K_{sat} estimates. The exercises discussed in section 4.3 showed that for events with below-threshold criteria (the sum of precipitation and ASI < 316 mm, Figure 4a), our field measurements and Darcy assumption were generally sufficient to account for the observed runoff response. However, for all above-threshold events, our estimates were significantly lower than the observed catchment runoff response, and Darcy velocities would need to be approximately an order of magnitude higher to account for the largest events. The assumptions made to perform these exercises were highly simplified and each simplification and assumption most likely overestimated hydrologic responses (e.g., flow paths oriented perpendicular to stream; stream channel flow routing assumed to be instantaneous). Therefore, better surface and subsurface flow representations (e.g., better hydraulic geometry, channel routing) would likely yield lower contributing areas and would further support our findings.

[32] We assume that hydraulic gradients in the shallow subsurface did not change significantly between events as variations in hydraulic gradient were limited by total soil depths which were significantly less than overall slope lengths. Hydraulic gradients could not realistically get much

steeper than the surface slope as seepage faces along stream channels were small (typically equivalent to surficial soil depths and <1 m), and if hydraulic gradients were significantly less than the surface slope, then the water table surface would drop into the lower soil horizons, which our data show to be uncorrelated with high stream flows. Therefore, Darcy velocities were most influenced by effective K_{sat}, which appeared to change significantly between below- and above-threshold events. We hypothesize that the change may have been due to water tables rising into highly transmissive flow paths in the near-surface soil horizons and/or a process change, such as macropore flow, which could not be accounted for by Darcian flow.

[33] The discontinuity between point- or plot-scale measurements of hydraulic conductivity and effective hydraulic conductivity at the hillslope scale has been long recognized [*Binley et al.*, 1989; *Bazemore et al.*, 1994; *Tani*, 1997; *Bonell*, 1998]. One possible explanation for this discontinuity is the integrated effect of preferential flow paths and macropore networks which have a tendency to self-organize and improve the overall drainage efficiency of a landscape, particularly as a system becomes wetter [*Sidle et al.*, 2001]. *Brooks et al.* [2004] studied an isolated trenched hillslope to examine the effective saturated hydraulic conductivity of a hillslope during snowmelt and rainfall events. Their results show that the effective K_{sat} was 1–2 orders of magnitude greater than small-scale measurements of K_{sat} based on soil core samples and a Guelph permeameter. They also note that the greatest discrepancy was in the surficial A horizon and found that the effective K_{sat} profile was best fit by a double exponential curve rather than a single exponential as is usually assumed (e.g., TOPMODEL [*Beven and Kirkby*, 1979]).

[34] In addition to the documented differences between effective K_{sat} values and point measurements, it is worth noting some conditions of our wells, which may have biased our slug test results toward low estimates of K_{sat}. As was mentioned in section 3.3, slug tests were performed at our site toward the end of snowmelt when water tables were relatively high. However, groundwater levels during large runoff events frequently exceeded the levels at which the slug tests were performed. Therefore, the slug tests did not represent the K_{sat} of the uppermost soil horizons which our permeameter data and *Brooks et al.* [2004] have shown to be significantly higher than in the lower and middle horizons. In addition, our wells had a screen length of 31 cm, and the lower edge of the screen was positioned to sit flush with the B/C interface. During slug tests, the depth of water in many wells was higher than the top of the screen, which may have also biased responses to be more representative of the lower and middle soil horizons. Both of these conditions may have had the effect of underrepresenting the effective K_{sat} of the integrated soil profile.

5.3. Overland Flow and Subsurface Stormflow

[35] In WS3, soil infiltration rates were sufficiently high that infiltration excess overland flow was not observed and was unlikely to occur under normal conditions at this site. In addition, evidence of saturation overland flow was not observed during site visits, and surface saturation was not reflected in any of the groundwater monitoring wells or soil moisture probes even during the largest events. Also, our
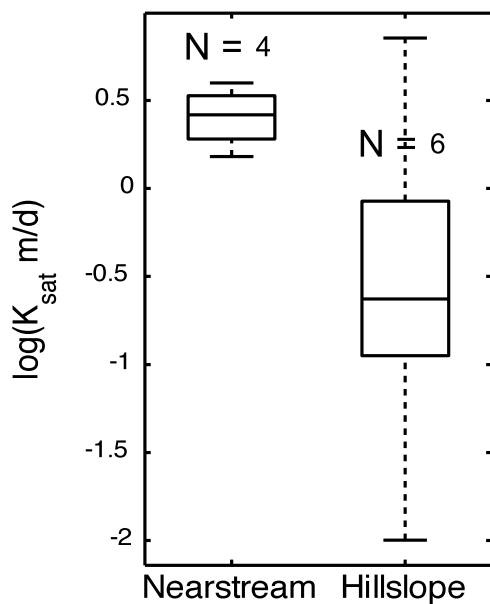
Figure 10. Box plot of saturated hydraulic conductivity as measured during rising head slug tests for near-stream and hillslope wells. Boxes represent the IQR of data, and whiskers describe the highest and lowest nonoutlier data. Outliers are defined as any data greater than 1.5 times IQR plus the third quartile or less than the first quartile minus 1.5 minus IQR.

results do not consistently support storm runoff generation via Darcian matrix flow, and we hypothesize that other forms of shallow subsurface stormflow and direct channel interception contribute to runoff in WS3. These results are consistent with previous hydrometric studies [*Pierce*, 1967; *Rosenthal*, 1986; *Stresky*, 1991; *Shattuck*, 1991; *Cedarholm*, 1994] and hydrochemical studies [*Hooper and Shoemaker*, 1986; *Hogan and Blum*, 2003; *Wellington and Driscoll*, 2004], which have shown that subsurface flow contributions to storm runoff are dominant at HBEF.

[36] While studies utilizing hydrograph separation and end-member mixing analysis have shown storm runoff at HBEF to be primarily composed of groundwater [*Hooper and Shoemaker*, 1986; *Wellington and Driscoll*, 2004], that result alone is not adequate to eliminate the possibility of saturation overland flow since return flows [*Dunne and Black*, 1970] may be old water sources. *Hogan and Blum* [2003] showed that during two rain events with contrasting runoff responses, the throughfall fraction of runoff (watershed 1, HBEF), as determined using isotope hydrograph separations, was comparable to the estimated volume of direct channel interception. Assuming that nearly all channel interception was translated to storm runoff, Hogan and Blum's results suggest that most new water contributions to stormflow occurred as direct channel interception and the balance of stormflow occurred as discharge of stored groundwater (e.g., by subsurface flow). If a significant saturation overland flow component were present, then we would expect to see an expanded surface-saturated area and consequently a larger volume of throughfall in stormflow, as would be predicted by the saturation overland flow model [*Dunne and Black*, 1970; *Crayosky et al.*, 1999] and has been seen at other sites where saturation overland flow oc-

curs [e.g., *Eshleman et al.*, 1993; *Shanley et al.*, 2002; *Kienzler and Naef*, 2008].

[37] The absence of classical saturation overland flow in WS3 can best be explained by the morphologic features of the near-stream zone. The watershed has little riparian area and is instead characterized by slopes which are only modestly concave in the immediate vicinity of the stream. We observed that stream water in the intermittent tributaries often reinfiltrated the streambed several meters upslope of the confluence with the main channel, suggesting relatively deeper water tables and/or more transmissive groundwater flow paths in the near-stream zones, which diverges from the saturation overland flow model. This characteristic was also supported by our observations that near-stream soils appeared to be structurally different from upslope soils. The near-stream areas had a higher fraction of gravel and rock fragments at depth, which we hypothesized to be relict buried alluvium (e.g., lag deposits), and hydraulic conductivities were typically an order of magnitude higher than in hillslope soils (Figure 10). The more transmissive soils in the near-stream zones may have served to quickly translate water to the stream channel, thus limiting water table heights and consequently any return flow.

5.4. Transmissivity Feedbacks

[38] Many well hydrographs displayed a curvilinear relationship with streamflow. Above an inflection point, small changes in groundwater levels were associated with a large change in streamflow, while below the inflection point, large changes in groundwater height were associated with small changes in streamflow. Similarly, our results also show a threshold production of quick flow depths based on maximum water table heights. One possible explanation for these groundwater-streamflow characteristics is that when water tables rose above a critical level in the soil profile, they entered soils with significantly higher K_{sat}, which increased subsurface stormflow rates. These characteristics are similar to the concept of transmissivity feedback [*Bishop*, 1991; *Kendall et al.*, 1999; *Bishop et al.*, 2004]. According to this theory, in certain glacial till soils, such as those at HBEF, as groundwater levels rise through the soil, profile transmissivity increases significantly. The increasingly transmissive flow paths increase the rate of drainage of groundwater, which reduces the rate of water table rise. This nonlinear behavior is an example of both a positive feedback (for transmissivity) as well as a form of self-limitation (for water table height), as discussed by *Phillips* [2003]. Our data show an apparent upper limit to hillslope water table rises (Figure 5) which may also support our hypothesis that transmissivity feedbacks occurred in WS3 and may offer another explanation of why saturation overland flow was uncommon in this environment (water tables were self-limiting).

5.5. Preferential Flow Paths

[39] We hypothesize that macropore flow may have also been an important process during large runoff events at WS3, particularly when water tables rose into near-surface soils. *Stresky* [1991] has shown that at HBEF the extent of soil pipes and macropores was most concentrated in the upper soil horizons and decreased significantly downward through the Bhs horizon. The layer of highest soil pipe

concentration was typically found in the upper ~10–30 cm of the soil profiles measured by Stresky which coincides with the upper limit of our observed water tables. In addition, Stresky used sprinkling experiments with dye tracers to show that flow through soil pipes (at the plot scale) interacted extensively with the surrounding soil matrix and occurred in both unsaturated and saturated conditions depending on precipitation rates, antecedent soil moisture, and depth to groundwater.

[40] Preferential flow through macropores has been shown to increase with antecedent wetness, to increase runoff yield, and to increase the effective contributing area to storm runoff [*Sidle et al.*, 1995; *Scherrer et al.*, 2007]. Discontinuous macropores also tend to organize into larger preferential flow systems as soil moisture increases [*Sidle et al.*, 2001]. These characteristics combined with *Stresky*'s [1991] observations of macropore and soil pipe distributions in HBEF soils could partially account for our inference of significantly higher effective K_{sat} during large runoff events with high soil moisture levels as well as support our hypothesis of a transmissivity feedback effect during runoff events with high water tables. Although *Laudon et al.* [2004] assert that the transmissivity feedback theory is based on flow through the soil matrix; it is not unreasonable to assume that similar effects could be seen with increased transmissivity caused by macropores in the upper soil horizons. We suggest that as soil moisture levels rose in watershed 3, the dominant flow processes may have shifted to create a more connected and efficient network of non-Darcian flow pathways, such as macropore flow through near-surface soils, thus allowing the much larger runoff response observed during above-threshold conditions.

[41] It is also worth mentioning that although we do not believe saturation overland flow is common at WS3, we did observe some discontinuous seep and return flow throughout the catchment, particularly in depressions and convergent areas, although these areas were spatially limited and water typically reinfiltrated the soil surface within a few meters of the seep origin. Although not detected by the monitoring network, it is possible that these areas may have expanded and/or become more connected during large runoff events. The development of a transient surface or near-surface flow path on hillslopes that could interact with the other flow mechanisms described may offer yet another explanation for our observed results.

6. Conclusions

[42] In watershed 3, storm runoff changed characteristically according to a soil moisture threshold identified by two independently measured indices. An antecedent soil moisture index (ASI) was determined from soil volumetric water content at four sites within one instrument transect, while a maximum water table height index was calculated from 28 shallow groundwater wells throughout the watershed. The sum of ASI and gross precipitation and the maximum water table height index both showed very similar threshold changes in total event quick flow volumes and were highly correlated for 13 runoff events considered in this study.

[43] Estimates of contributing areas and lateral subsurface flows based on field measurements of saturated hydraulic conductivity suggest that Darcian matrix flows and channel interception can only partially explain the observed catchment runoff responses. During runoff events with above-threshold criteria the effective saturated hydraulic conductivity of the catchment significantly exceeded our field measurements, suggesting that our field measurements were unrepresentative of the system and/or non-Darcian subsurface flow processes were important during these events. We observed that groundwater fluctuations throughout the catchment became increasingly synchronized with streamflow as the runoff response increased. In addition, the groundwater-streamflow relationship for many wells showed that above critical depths small changes in groundwater levels were correlated with large changes in streamflow. The above results, combined with the threshold change in stormflow as a function of soil water storages, led us to conclude that as the system wetted up, a characteristic change in runoff production occurred. This change likely reflected subsurface stormflow processes which were sensitive to the spatial distribution and connectivity of shallow groundwater and increased with overall catchment wetness. A transmissivity feedback mechanism and/or non-Darcian preferential flows through near-surface macropore networks would be dependent on the above criteria and might provide a process based explanation of our observed results.

[44] These results offer insight into the complex interactions of processes at the scale of a small catchment by revealing relatively simple and predictable patterns arising from nonlinear controls. Our work emphasizes (1) the need to consider a threshold change in process representation and (2) the importance of estimating soil water storage capacity and catchment-averaged water table depths when describing the stream response of a till-mantled catchment dominated by shallow flow systems.

References

Amoozegar, A. (1989), A compact constant-head permeameter for measuring saturated hydraulic conductivity of the vadose zone, *Soil Sci. Soc. Am. J.*, *53*, 1356–1361.

Bailey, A. S., J. W. Hornbeck, J. L. Campbell, and C. Eagar (2003), Hydrometeorological database for Hubbard Brook Experimental Forest: 1955–2000, *Gen. Tech. Rep. NE-305*, 36 pp., U.S. Dep. of Agric., For. Serv., Northeast. Res. Stn., Newtown Square, Pa.

Band, L. E., P. Patterson, R. Nemani, and S. W. Running (1993), Forest ecosystem processes at the watershed scale: Incorporating hillslope hydrology, *Agric. For. Meteorol.*, *63*(1–2), 93–126, doi:10.1016/0168-1923(93)90024-C.

Bazemore, D. E., K. N. Eshleman, and K. J. Hollenbeck (1994), The role of soil water in stormflow generation in a forested headwater catchment: Synthesis of natural tracer and hydrometric evidence, *J. Hydrol.*, *162*(1–2), 47–75, doi:10.1016/0022-1694(94)90004-3.

Beven, K., and P. Germann (1982), Macropores and water flow in soils, *Water Resour. Res.*, *18*(5), 1311–1325, doi:10.1029/WR018i005p01311.

Beven, K. J., and M. J. Kirkby (1979), A physically based, variable contributing area model of basin hydrology, *Hydrol. Sci. Bull.*, *24*(1), 43–69, doi:10.1080/02626667909491834.

Binley, A., K. Beven, and J. Elgy (1989), A physically based model of heterogeneous hillslopes: 2. Effective hydraulic conductivities, *Water Resour. Res.*, *25*(6), 1227–1233, doi:10.1029/WR025i006p01227.

Bishop, K. (1991), Episodic increases in stream acidity, catchment flow pathways and hydrograph separation, Ph.D. thesis, 246 pp., Univ. of Cambridge, Cambridge, U. K.

Bishop, K., J. Seibert, S. Köhler, and H. Laudon (2004), Resolving the double paradox of rapidly mobilized old water with highly variable responses in runoff chemistry, *Hydrol. Processes*, 18(1), 185–189, doi:10.1002/hyp.5209.

Bonell, M. (1998), Selected challenges in runoff generation research in forests from the hillslope to headwater drainage basin scale, *J. Am. Water Resour. Assoc.*, 34(4), 765–785, doi:10.1111/j.1752-1688.1998.tb01514.x.

Bormann, F. H., and G. E. Likens (1967), Nutrient cycling, *Science*, 155(3761), 424–429, doi:10.1126/science.155.3761.424.

Brooks, E. S., J. Boll, and P. A. McDaniel (2004), A hillslope-scale experiment to measure lateral saturated hydraulic conductivity, *Water Resour. Res.*, 40, W04208, doi:10.1029/2003WR002858.

Buttle, J. M., P. J. Dillon, and G. R. Eerkes (2004), Hydrologic coupling of slopes, riparian zones and streams: An example from the Canadian Shield, *J. Hydrol.*, 287(1–4), 161–177, doi:10.1016/j.jhydrol.2003.09.022.

Carey, S. K., and W. L. Quinton (2005), Evaluating runoff generation during summer using hydrometric, stable isotope and hydrochemical methods in a discontinuous permafrost alpine catchment, *Hydrol. Processes*, 19(1), 95–114, doi:10.1002/hyp.5764.

Cedarholm, D. (1994), Dominant soil water pathways on a northern New England forested hillslope, M.S. thesis, 177 pp., Univ. of N. H., Durham.

Crayosky, T. W., D. R. Dewalle, T. A. Seybert, and T. E. Johnson (1999), Channel precipitation dynamics in a forested Pennsylvania headwater catchment (USA), *Hydrol. Processes*, 13(9), 1303–1314, doi:10.1002/(SICI)1099-1085(19990630)13:9<1303::AID-HYP815>3.0.CO;2-P.

DeWalle, D. R., B. R. Swistock, and W. E. Sharpe (1988), Three-component tracer model for stormflow on a small Appalachian forested catchment, *J. Hydrol.*, 104(1–4), 301–310, doi:10.1016/0022-1694(88)90171-0.

Dickinson, W. T., and H. Whiteley (1970), Watershed areas contributing to runoff, paper presented at International Symposium on the Results of Research on Representative and Experimental Basins, Int. Assoc. of Hydrol. Sci., Wellington.

Dunne, T. (1983), Relation of field studies and modeling in the prediction of storm runoff, *J. Hydrol.*, 65(1–3), 25–48, doi:10.1016/0022-1694(83)90209-3.

Dunne, T., and R. D. Black (1970), An experimental investigation of runoff production in permeable soils, *Water Resour. Res.*, 6(2), 478–490, doi:10.1029/WR006i002p00478.

Eshleman, K. N., J. S. Pollard, and A. K. O'Brien (1993), Determination of contributing areas for saturation overland flow from chemical hydrograph separations, *Water Resour. Res.*, 29(10), 3577–3587, doi:10.1029/93WR01811.

Federer, C. A. (1969), New landmark in the White Mountains, *Appalachia*, 12, 589–594.

Fujimoto, M., N. Ohte, and M. Tani (2008), Effects of hillslope topography on hydrological responses in a weathered granite mountain, Japan: Comparison of the runoff response between the valley-head and the side slope, *Hydrol. Processes*, 22(14), 2581–2594, doi:10.1002/hyp.6857.

Grayson, R. B., I. D. Moore, and T. A. McMahon (1992), Physically based hydrologic modeling: 2. Is the concept realistic?, *Water Resour. Res.*, 28(10), 2659–2666, doi:10.1029/92WR01259.

Haga, H., Y. Matsumoto, J. Matsutani, M. Fujita, K. Nishida, and Y. Sakamoto (2005), Flow paths, rainfall properties, and antecedent soil moisture controlling lags to peak discharge in a granitic unchanneled catchment, *Water Resour. Res.*, 41, W12410, doi:10.1029/2005WR004236.

Harr, R. D. (1977), Water flux in soil and subsoil on a steep forested slope, *J. Hydrol.*, 33(1–3), 37–58, doi:10.1016/0022-1694(77)90097-X.

Hewlett, J. D., and A. R. Hibbert (1967), Factors affecting the response of small watersheds to precipitation in humid areas, in *International Symposium on Forest Hydrology*, edited by W. E. Sopper and H. W. Lull, pp. 275–291, Pergamon, New York.

Hewlett, J. D., and W. L. Nutter (1970), Varying source area of streamflow from upland basins, in *Symposium on Interdisciplinary Aspects of Watershed Management*, edited by G. L. Martin, pp. 65–83, *Am. Soc. of Civ. Eng.*, New York.

Hjerdt, K. N. (2002), Deconvoluting the hydrologic response of a small till catchment: Spatial variability of groundwater level and quality in relation to streamflow, Ph.D. thesis, 204 pp., State Univ. of N. Y. Coll. of Environ. Sci. and For., Syracuse.

Hogan, J. F., and J. D. Blum (2003), Tracing hydrologic flow paths in a small forested watershed using variations in $^{87}Sr/^{86}Sr$, [Ca]/[Sr], [Ba]/[Sr] and $\delta^{18}O$, *Water Resour. Res.*, 39(10), 1282, doi:10.1029/2002WR001856.

Hooper, R. P., and C. A. Shoemaker (1986), A comparison of chemical and isotopic hydrograph separation, *Water Resour. Res.*, 22(10), 1444–1454, doi:10.1029/WR022i010p01444.

Hooper, R. P., B. T. Aulenbach, D. A. Burns, J. McDonnell, J. Freer, C. Kendall, and K. Beven (1998), Riparian control of stream-water chemistry: Implications for hydrochemical basin models, in *Hydrology, Water Resources and Ecology in Headwaters HeadWater'98*, edited by K. Kovar et al., pp. 451–458, Int. Assoc. of Hydrol. Sci., Oxfordshire, U. K.

Hornbeck, J. W. (1973), Storm flow from hardwood-forested and cleared watersheds in New Hampshire, *Water Resour. Res.*, 9(2), 346–354, doi:10.1029/WR009i002p00346.

Hornbeck, J. W. (1975), Streamflow response to forest cutting and revegetation, *Water Resour. Bull.*, 11(6), 1257–1260.

Hornbeck, J. W., R. S. Pierce, and C. A. Federer (1970), Streamflow changes after forest clearing in New England, *Water Resour. Res.*, 6(4), 1124–1132, doi:10.1029/WR006i004p01124.

Hornbeck, J. W., C. W. Martin, R. S. Pierce, F. H. Bormann, G. E. Likens, and J. S. Eaton (1986), Clearcutting northern hardwoods: Effects on hydrologic and nutrient ion budgets, *For. Sci.*, 32(3), 667–686.

Hornbeck, J. W., C. W. Martin, and C. Eagar (1997), Summary of water yield experiments at Hubbard Brook Experimental Forest, New Hampshire, *Can. J. For. Res.*, 27(12), 2043–2052, doi:10.1139/cjfr-27-12-2043.

James, A. L., and N. T. Roulet (2007), Investigating hydrologic connectivity and its association with threshold change in runoff response in a temperate forested watershed, *Hydrol. Processes*, 21(25), 3391–3408, doi:10.1002/hyp.6554.

Johnson, C. E., C. T. Driscoll, T. G. Siccama, and G. E. Likens (2000), Element fluxes and landscape position in a northern hardwood forest watershed ecosystem, *Ecosystems*, 3(2), 159–184, doi:10.1007/s100210000017.

Kendall, K. A., J. B. Shanley, and J. J. McDonnell (1999), A hydrometric and geochemical approach to test the transmissivity feedback hypothesis during snowmelt, *J. Hydrol.*, 219(3–4), 188–205, doi:10.1016/S0022-1694(99)00059-1.

Kienzler, P. M., and F. Naef (2008), Subsurface storm flow formation at different hillslopes and implications for the 'old water paradox,' *Hydrol. Processes*, 22(1), 104–116, doi:10.1002/hyp.6687.

Kim, H. J., R. C. Sidle, R. D. Moore, and R. Hudson (2004), Throughflow variability during snowmelt in a forested mountain catchment, coastal British Columbia, Canada, *Hydrol. Processes*, 18(7), 1219–1236, doi:10.1002/hyp.1396.

Kim, H. J., R. C. Sidle, and R. D. Moore (2005), Shallow lateral flow from a forested hillslope: Influence of antecedent wetness, *Catena*, 60, 293–306, doi:10.1016/j.catena.2004.12.005.

Kirchner, J. W. (2003), A double paradox in catchment hydrology and geochemistry, *Hydrol. Processes*, 17(4), 871–874, doi:10.1002/hyp.5108.

Kizito, F., C. S. Campbell, G. S. Campbell, D. R. Cobos, B. L. Teare, B. Carter, and J. W. Hopmans (2008), Frequency, electrical conductivity and temperature analysis of a low-cost capacitance soil moisture sensor, *J. Hydrol.*, 352(3–4), 367–378.

Kohler, M. A., and R. K. Linsley (1951), Predicting the runoff from storm rainfall, *Res. Pap. 34*, U.S. Weather Bur., Washington, D. C.

Laudon, H., J. Seibert, S. Köhler, and K. Bishop (2004), Hydrological flow paths during snowmelt: Congruence between hydrometric measurements and oxygen 18 in meltwater, soil water, and runoff, *Water Resour. Res.*, 40, W03102, doi:10.1029/2003WR002455.

Lehmann, P., C. Hinz, G. McGrath, H. J. Tromp-van Meerveld, and J. J. McDonnell (2007), Rainfall threshold for hillslope outflow: An emergent property of flow pathway connectivity, *Hydrol. Earth Syst. Sci.*, 11(2), 1047–1063, doi:10.5194/hess-11-1047-2007.

Leonard, R. E. (1961a), Interception of precipitation by northern hardwoods, *Stn. Pap. NE-159*, 16 pp., U.S. Dep. of Agric., For. Serv., Northeast. For. Exp. Stn., Upper Darby, Pa.

Leonard, R. E. (1961b), Net precipitation in a northern hardwood forest, *J. Geophys. Res.*, 66, 2417–2421, doi:10.1029/JZ066i008p02417.

Likens, G. E., and F. H. Bormann (1995), *Biogeochemistry of a Forested Ecosystem*, 159 pp., Springer, New York.

Likens, G. E., F. H. Bormann, N. M. Johnson, D. W. Fisher, and R. S. Pierce (1970), Effects of forest cutting and herbicide treatment on nutrient budgets in the Hubbard Brook Watershed-Ecosystem, *Ecol. Monogr.*, 40(1), 23–47, doi:10.2307/1942440.

Likens, G. E., C. T. Driscoll, and D. C. Buso (1996), Long-term effects of acid rain: Response and recovery of a forest ecosystem, *Science*, 272, 244–246, doi:10.1126/science.272.5259.244.

Lynch, J. A., E. S. Corbett, and W. E. Sopper (1979), Effects of antecedent soil moisture on stormflow volumes and timing, in *Modeling Hydrologic Processes: Proceedings of the Fort Collins Third International Hydrology Symposium, on Theoretical and Applied Hydrology, Held at Colorado State University, Fort Collins, Colorado, USA, July 27–29, 1977*, edited by H. J. Morel-Seytoux, pp. 89–99, Water Resour. Publ., Fort Collins, Colo.

McDonnell, J. J. (1990), A rationale for old water discharge through macropores in a steep, humid catchment, *Water Resour. Res.*, 26(11), 2821–2832, doi:10.1029/WR026i011p02821.

McDonnell, J. J. (2003), Where does water go when it rains? Moving beyond the variable source area concept of rainfall-runoff response, *Hydrol. Processes*, 17(9), 1869–1875, doi:10.1002/hyp.5132.

McDonnell, J. J., et al. (2007), Moving beyond heterogeneity and process complexity: A new vision for watershed hydrology, *Water Resour. Res.*, 43, W07301, doi:10.1029/2006WR005467.

McGlynn, B. L., J. J. McDonnell, and D. D. Brammer (2002), A review of the evolving perceptual model of hillslope flowpaths at the Maimai catchments, New Zealand, *J. Hydrol.*, 257(1–4), 1–26, doi:10.1016/S0022-1694(01)00559-5.

Mosley, M. P. (1979), Streamflow generation in a forested watershed, New Zealand, *Water Resour. Res.*, 15(4), 795–806, doi:10.1029/WR015i004p00795.

Noether, G. E. (1991), *Introduction to Statistics: The Nonparametric Way*, 414 pp., Springer, New York.

Pan, F., and C. D. Peters-Lidard (2008), On the relationship between mean and variance of soil moisture fields, *J. Am. Water Resour. Assoc.*, 44(1), 235–242, doi:10.1111/j.1752-1688.2007.00150.x.

Penna, D., M. Borga, D. Norbiato, and G. Dalla Fontana (2009), Hillslope scale soil moisture variability in a steep alpine terrain, *J. Hydrol.*, 364(3–4), 311–327, doi:10.1016/j.jhydrol.2008.11.009.

Phillips, J. D. (2003), Sources of nonlinearity and complexity in geomorphic systems, *Prog. Phys. Geogr.*, 27(1), 1–23, doi:10.1191/0309133303pp340ra.

Pierce, R. S. (1967), Evidence of overland flow on forest watersheds, in *International Symposium on Forest Hydrology*, edited by W. E. Sopper and H. W. Lull, pp. 247–251, Pergamon, New York.

Redding, T. E., and K. J. Devito (2008), Lateral flow thresholds for aspen forested hillslopes on the Western Boreal Plain, Alberta, Canada, *Hydrol. Processes*, 22(21), 4287–4300, doi:10.1002/hyp.7038.

Rosenthal, G. (1986), Some observations on the mechanisms of hillslope runoff at Hubbard Brook Experimental Forest, West Thornton, New Hampshire, M.S. thesis, 222 pp., Cornell Univ., Ithaca, N. Y.

Scherrer, S., F. Naef, A. O. Faeh, and I. Cordery (2007), Formation of runoff at the hillslope scale during intense precipitation, *Hydrol. Earth Syst. Sci.*, 11(2), 907–922, doi:10.5194/hess-11-907-2007.

Seibert, J., K. Bishop, A. Rodhe, and J. J. McDonnell (2003), Groundwater dynamics along a hillslope: A test of the steady state hypothesis, *Water Resour. Res.*, 39(1), 1014, doi:10.1029/2002WR001404.

Shanley, J. B., C. Kendall, T. E. Smith, D. M. Wolock, and J. J. McDonnell (2002), Controls on old and new water contributions to stream flow at some nested catchments in Vermont, USA, *Hydrol. Processes*, 16(3), 589–609, doi:10.1002/hyp.312.

Shattuck, P. C. (1991), Shallow water-table response to precipitation and evapotranspiration in an ephemeral stream valley, Woodstock, New Hampshire, M.S. thesis, 113 pp., Univ. of N. H., Durham.

Sidle, R. C., and Y. Onda (2004), Hydrogeomorphology: Overview of an emerging science, *Hydrol. Processes*, 18(4), 597–602, doi:10.1002/hyp.1360.

Sidle, R. C., Y. Tsuboyama, S. Noguchi, I. Hosoda, M. Fujieda, and T. Shimizu (1995), Seasonal hydrologic response at various spatial scales in a small forested catchment, Hitachi Ohta, Japan, *J. Hydrol.*, 168(1–4), 227–250, doi:10.1016/0022-1694(94)02639-S.

Sidle, R. C., S. Noguchi, Y. Tsuboyama, and K. Laursen (2001), A conceptual model of preferential flow systems in forested hillslopes: Evidence of self-organization, *Hydrol. Processes*, 15(10), 1675–1692, doi:10.1002/hyp.233.

Sivapalan, M. (2003), Process complexity at hillslope scale, process simplicity at the watershed scale: Is there a connection?, *Hydrol. Processes*, 17(5), 1037–1041, doi:10.1002/hyp.5109.

Sklash, M. G., and R. N. Farvolden (1979), The role of groundwater in storm runoff, *J. Hydrol.*, 43(1–4), 45–65, doi:10.1016/0022-1694(79)90164-1.

Stresky, S. J. (1991), Morphology and flow characteristics of pipes in a forested New England hillslope, M.S. thesis, 131 pp., Univ. of N. H., Durham.

Tani, M. (1997), Runoff generation processes estimated from hydrological observations on a steep forested hillslope with a thin soil layer, *J. Hydrol.*, 200(1–4), 84–109, doi:10.1016/S0022-1694(97)00018-8.

Tetzlaff, D., J. J. McDonnell, S. Uhlenbrook, K. J. McGuire, P. W. Bogaart, F. Naef, A. J. Baird, S. M. Dunn, and C. Soulsby (2008), Conceptualizing catchment processes: Simply too complex?, *Hydrol. Processes*, 22(11), 1727–1730, doi:10.1002/hyp.7069.

Tromp-van Meerveld, H. J., and J. J. McDonnell (2006a), Threshold relations in subsurface stormflow: 2. The fill and spill hypothesis, *Water Resour. Res.*, 42, W02411, doi:10.1029/2004WR003800.

Tromp-van Meerveld, H. J., and J. J. McDonnell (2006b), Threshold relations in subsurface stormflow: 1. A 147-storm analysis of the Panola hillslope, *Water Resour. Res.*, 42, W02410, doi:10.1029/2004WR003778.

Turton, D. J., C. T. Haan, and E. L. Miller (1992), Subsurface flow responses of a small forested catchment in the Ouachita Mountains, *Hydrol. Processes*, 6(1), 111–125, doi:10.1002/hyp.3360060110.

Uchida, T., K. Kosugi, and T. Mizuyama (1999), Runoff characteristics of pipeflow and effects of pipeflow on rainfall-runoff phenomena in a mountainous watershed, *J. Hydrol.*, 222(1–4), 18–36, doi:10.1016/S0022-1694(99)00090-6.

U.S. Department of Agriculture Forest Service (1996), Hubbard Brook ecosystem study: Site description and research activities, *Publ. NE-INF-96-96R*, 2nd ed., 53 pp., Northeast. For. Exp. Stn., Newtown Square, Pa.

U.S. Soil Conservation Service (1969), *SCS National Engineering Handbook, Section 4: Hydrology*, U.S. Gov. Print. Off., Washington, D. C.

Weight, W. D., and J. L. Sonderegger (2001), *Manual of Applied Field Hydrogeology*, 608 pp., McGraw-Hill, New York.

Weiler, M., and F. Naef (2003), An experimental tracer study of the role of macropores in infiltration in grassland soils, *Hydrol. Processes*, 17(2), 477–493, doi:10.1002/hyp.1136.

Wellington, B. I., and C. T. Driscoll (2004), The episodic acidification of a stream with elevated concentrations of dissolved organic carbon, *Hydrol. Processes*, 18(14), 2663–2680, doi:10.1002/hyp.5574.

Wels, C., C. H. Taylor, J. R. Cornett, and B. D. Lazerte (1991), Streamflow generation in a headwater basin on the precambrian shield, *Hydrol. Processes*, 5(2), 185–199, doi:10.1002/hyp.3360050206.

Western, A., R. Grayson, G. Blöschl, and D. Wilson (2003), Spatial variability of soil moisture and its implications for scaling, in *Scaling Methods in Soil Physics*, edited by Y. Pachepsky, D. E. Radcliffe, and H. M. E. Selim, pp. 120–142, CRC Press, Boca Raton, Fla.

Williams, A. G., J. F. Dowd, and E. W. Meyles (2002), A new interpretation of kinematic stormflow generation, *Hydrol. Processes*, 16(14), 2791–2803, doi:10.1002/hyp.1071.

J. M. Detty, Center for the Environment, Plymouth State University, MSC63 17 High St., Plymouth, NH 03264, USA.

K. J. McGuire, Department of Forest Resources and Environmental Conservation, Virginia Water Resources Research Center, Virginia Polytechnic Institute and State University, 210B Cheatham Hall (0444), Blacksburg, VA 24061, USA. (kevin.mcguire@vt.edu)